ISSN 0018-151X, High Temperature, 2008, Vol. 46, No. 1, pp. 60–68. © Pleiades Publishing, Ltd., 2008.
Original Russian Text © O.A. Novruzova, A.E. Galashev, 2008, published in Teplofizika Vysokikh Temperatur, Vol. 46, No. 1, 2008, pp. 66–75.

THERMOPHYSICAL PROPERTIES OF MATERIALS

Numerical Simulation of IR Absorption, Reflection, and Scattering in Dispersed Water–Oxygen Media

O. A. Novruzova and A. E. Galashev

Institute of Environmental Engineering, Ural Division, Russian Academy of Sciences, Ekaterinburg, 620219 Russia

Received July 25, 2006

Abstract—The method of molecular dynamics along with the flexible model of molecules are used to study the spectral characteristics of systems of clusters of $(H_2O)_n$, $(O_2)_m(H_2O)_n$, and $(O)_i(H_2O)_n$, $m \le 2$, $i \le 4$, $10 \le n \le 50$. It is demonstrated that the integral intensity of absorption of IR radiation decays after water clusters adsorb oxygen. In addition, the adsorption of oxygen causes a significant decrease in the reflection coefficient R of monochromatic IR radiation. In so doing, the $R(\omega)$ spectrum splits into bands and exhibits seven peaks in the frequency region of $0 \le \omega \le 3500$ cm^{-1}. The dissociation of oxygen molecules captured by clusters makes the peaks of $R(\omega)$ spectrum more resolved. The attachment of molecular oxygen by clusters leads to decay of the power of their IR radiation, while the capture of atomic oxygen, on the contrary, is accompanied by an increase in the rate of dissipation of energy accumulated by water aggregates.

PACS numbers: 33.20Ea; 36.40 Vz

DOI: 10.1134/S0018151X08010094

INTRODUCTION

The flux of ultraviolet (UV) solar radiation, which carries about 1% of the incoming solar energy, comes to altitudes of 20–40 km, where it is absorbed by ozone to cause its dissociation. However, a large fraction of energy of UV radiation dissipates at altitudes of 80–100 km and causes dissociation of molecular oxygen. Above 100 km, hard UV radiation performs the primary ionization of the atmosphere, as well as its heating. In this region, the temperature increases with altitude, and its variation is defined both by heating due to UV radiation and by heat removal downwards by molecular and turbulent thermal conductivity.

One of the natural sources of oxygen may be provided by water. The effect of UV radiation on water results in the generation of atomic and molecular oxygen and hydrogen in the upper atmosphere of the Earth (above the ozone layer). Lighter-than-air hydrogen escapes from the terrestrial atmosphere, and oxygen, on the contrary, stays there [1]. In general, the properties of natural water largely depend on oxygen it contains. The presence of calcite, magnesium, and other solutes in water leads to the binding of a part of oxygen. The concentrations of these substances may be most different; therefore, one must expect an even greater diversity of properties in the case of water saturated with oxygen. Dissolved oxygen and calcite make water a magnetic medium [2]. The observed paramagnetism is largely due to the presence of uncompensated magnetic moments which arise because of oxygen. As a rule, the nature of these moments is associated with the orbital motion of electrons, their spin.

Water clusters formed owing to hydrogen bonds are rather stable formations. These clusters exhibit a high capacity for adsorbing molecules of other gases. For example, it was experimentally found that water clusters with a size of up to nine atoms are capable of capturing and holding a benzene molecule whose molecular weight is half the weight of such cluster [3]. Previously, the method of molecular dynamics in the approximation of hard TIP4P model of water was used to demonstrate [4] that, as a result of the attachment of O_2 molecules to $(H_2O)_n$ clusters, the absorption coefficient decreases, and reflection coefficient increases. The effect of adsorption of oxygen on the spectral characteristics of water clusters must be reflected more accurately when using the flexible model of molecules.

It is the objective of this study to use the flexible model of molecules for studying the capture of molecular and atomic oxygen by water clusters and determining the effect of oxygen adsorption by dispersed water medium on the absorption spectra of IR radiation and reflection, as well as for finding out how the power of radiation of cluster systems varies in so doing.

COMPUTATIONAL MODEL

The extensively employed computer models of water SPC [5], SPC/E [6], and TIP3P and TIP4P [7] reproduce the gas-phase properties of water and properties of ice in a wide range of thermodynamic parameters much better than the properties of liquid water. We used a refined TIP4P model of water [8]. Dang and Chang [8] changed significantly the parameters of the Lennard–Jones part of potential, so that the coefficients

with the terms characterizing repulsion and attraction were reduced by factors 2.5 and 2.9, respectively. In addition, the center of localization of negative charge in this model is located at a distance of 0.0215 nm from the center of oxygen atom instead of 0.015 nm previously. This made possible the correction of permanent dipole moment of water molecule to a value of 1.848 D which corresponds to the experimentally obtained value of this quantity in the gas phase. The dynamics of system of molecules were realized with water-water intermolecular interaction potential [9] and with description of oxygen-oxygen and oxygen-water interaction in the form of the sum of repulsion and dispersion contributions [10],

$$\Phi(r_{ij}) = b_i b_j \exp[-(c_i + c_j) r_{ij}] - a_i a_j r_{ij}^{-6},$$

where the parameters a_i, b_i, and c_i of the potential describing these interactions were borrowed from [11]. The potentials employed for pairs (O–O, O–H, H–H) of interacting atoms are given in Fig. 1. Each of these potentials has an attraction region and a repulsion region. The transition from repulsion to attraction is observed at 0.34, 0.37, and 0.42 nm for atomic pairs of O–O, O–H, and H–H, respectively. The O–O pair has the steepest repulsion branch, and the softest repulsion is exhibited by the H–H pair.

Strict flexible models of water cannot be purely classical; they must include quantum degrees of freedom into consideration [12]. However, the inclusion of quantum effects causes an increase in the amount of computations by at least an order of magnitude and makes the simulation inefficient.

Flexible models of molecules within the Hamilton dynamics were further developed in [13, 14]. We will consider a diatomic molecule. Let atoms a and b in the molecule be spaced at

$$q = \|\mathbf{r}_a - \mathbf{r}_b\|,$$

where $\mathbf{r}_a$ and $\mathbf{r}_b$ are vectors defining the positions of atoms. We use $\mathbf{v}_a$ and $\mathbf{v}_b$ to represent the respective velocities, and write the reduced mass as

$$\mu = \frac{m_a m_b}{m_a + m_b}.$$

The size of molecules represented by atoms a and b is defined by balancing out the total potential force $\mathbf{f}(\mathbf{q}) = -\dfrac{\partial \mathbf{r}}{\partial \mathbf{q}} \nabla\Phi(\mathbf{r})$ by the centrifugal force $-\mu q\omega^2$ so that

$$-\mu q\omega^2 - \mathbf{f}(\mathbf{r})\frac{\partial \mathbf{r}}{\partial \mathbf{q}} = 0,$$

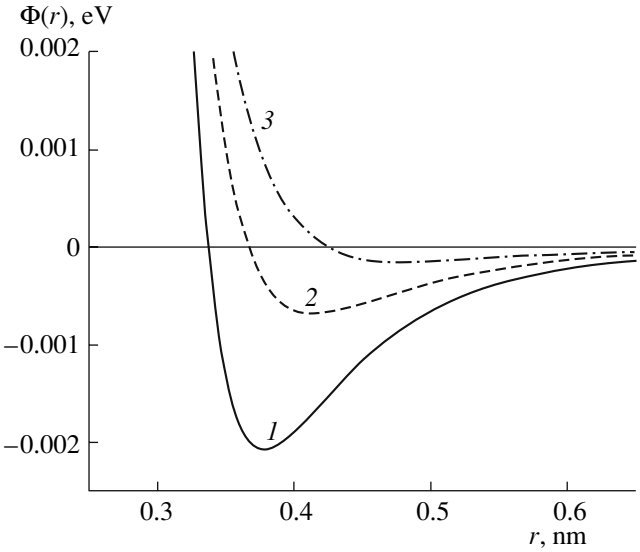

Fig. 1. Potentials of interaction of atomic pairs: (*1*) O–O, (*2*) O–H, (*3*) H–H.

where $\omega = \|\mathbf{v}_a - \mathbf{v}_b\|/q$ is the angular velocity. We use the minimization of contribution made by each generalized coordinate to potential energy U and derive

$$\frac{\partial}{\partial q_i} H(\mathbf{r}, \mathbf{v}) = \frac{\partial}{\partial q_i}\left(\frac{1}{2}\mu_i q_i^2 \omega_i^2 + U(\mathbf{r})\right) = 0.$$

This method is generalized to molecules of any composition [12].

The investigation of adsorption of oxygen by water clusters was started by developing a configuration consisting of an equilibrium water cluster and surrounding molecules (atoms) of oxygen. The initial equilibrium configurations of water clusters were obtained in separate molecular-dynamic calculations, with the kinetic energy of molecules which made up the cluster corresponding to a temperature of 233 K. The center of free molecule of oxygen was initially located at a distance of 0.6–0.7 nm from the nearest center of water molecule entering the composition of cluster. As a result, each oxygen molecule found itself in the field of molecular interaction. The cut-off radius of all interactions in the model was 0.9 nm. The linear molecule of O_2 was oriented along the ray connecting its center with the cluster center of mass. In the case of two molecules attached to the cluster, they were located along one and the same ray but on different sides of the cluster.

Similar to this was the initial arrangement of oxygen atoms in the vicinity of water cluster, except that there was no need for orienting spherically symmetric atoms. In the case of four oxygen atoms, they were located on normally intersecting lines. The point of intersection of

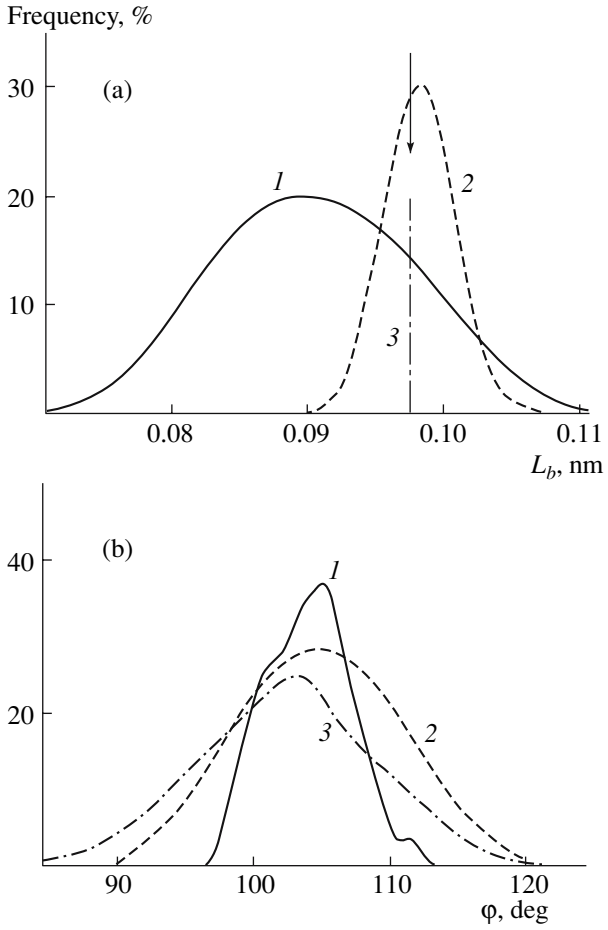

Fig. 2. The distributions of (a) lengths of intramolecular bonds and (b) angles: (*1*) our model for H_2O molecules in $(O)_4(H_2O)_{50}$ cluster, (*2*) MCDHO flexible model of water molecules [21], (*3*) BJH model (supercritical state) [18].

the lines coincided with the cluster center of mass. Each atom was located on its ray issuing from this center. This symmetric arrangement of molecules (atoms) developed conditions of uniform impact of impurity on the cluster and reduced to a minimum the interaction between O_2 or O being held.

The balancing of the newly formed system was performed in the time interval of $0.6 \times 10^6 \Delta t$ with the time step $\Delta t = 10^{-17}$ s, and then the desired physicochemical properties were calculated in the interval of $2 \times 10^6 \Delta t$. The fourth-order Gear method was used for integrating the equations of motion of centers of mass of molecules [15]. The analytical solution of equations of motion for rotation of molecules was performed using the Rodrigues–Hamilton parameters [16], and the scheme of integration of equations of motion in the presence of rotations corresponded to the approach suggested by Sonnenschein [17]. The computations were performed in a Pentium-IV computer with the processor clock frequency of 3.8 GHz.

PHYSICAL PROPERTIES OF FLEXIBLE MODEL OF MOLECULES

Flexible models of molecules offer a significant advantage in that they enable one to investigate the effect of temperature, pressure, and local environment of molecules and ions on characteristics such as dipole moments and vibration frequencies. Their application for simulation of water systems is especially useful from the standpoint of interpreting the effect of chemical composition, revealing the structural features, and determining more accurately the thermodynamic properties.

In [18], the BJH (Bopp–Jancso–Heinzinger) flexible model of water was used for analysis of intramolecular valence and deformation vibrations in the supercritical region of water. The interatomic potential of this model, which describes the internal degrees of freedom of molecule, is represented as a linear combination of double, triple, and quadruple products of differences made up for distances and angles which characterize the geometry of molecule. A red shift of valence vibration frequency of water relative to the respective characteristics of the gas phase was revealed, as well as a blue shift of deformation vibration frequency upon an increase in the density of water. These data agree with the behavior of experimentally obtained Raman spectra [19, 20]. A more perfect MCDHO flexible model of water molecule involves the use of the Morse potential for preassigning fluctuations of OH distances and of the quadratic polynomial for simulating the buckling of molecule as a result of variation of the HOH angle [21]. In this model, the polarizability of molecule is attained owing to mobile charge whose position is defined by the minimization of energy for the preassigned configuration of atoms.

Comparison of the flexible model employed by us with the MCDHO and BJH models of water is made in Fig. 2, which gives the distributions of intramolecular length L_b of the bond of OH and angle $\varphi = \angle(\mathrm{HOH})$. The characteristics of L_b and φ for an isolated water molecule are defined as $L_b^f(\mathrm{OH}) = 0.09572$ nm and $\angle(\mathrm{HOH})^f = 104.52°$. The distribution of length L_b of H_2O molecules in $(O)_4(H_2O)_n$ cluster is characterized by fairly wide peak, and the position of its maximum shifts to the left by ~0.007 nm relative to $L_b^f(\mathrm{OH})$. Corresponding to the most probable value of parameter L_b in MCDHO is 0.09828 nm, i.e., the OH bond more often turns out to be stretched relative to L_b^f. The distribution of bond length in this model exhibits a much lower dispersion than that in the case of model employed for clusters investigated by us. For the BJH model of water, the average value of L_b was 0.09755 nm. This quantity is marked by arrow in Fig. 2a, because the pattern of distribution of L_b is not given in [18]. The distribution of HOH angle for the models under consideration is given in Fig. 2b. In the case of $(O)_4(H_2O)_{50}$ cluster, the

distribution of angles φ is diffuse, asymmetric, and has a maximum in the vicinity of angle ~106°. The distribution of angles φ for the MCDHO model is almost symmetric, and the most probable value of HOH angle exceeds the value of $\angle(\mathrm{HOH})^f$ by only 0.48°. However, the dispersion of this distribution exceeds significantly the similar characteristic for the φ-distribution of clusters under investigation. The angular distribution of the BJH model of water with a maximum at 100.78° exhibits an even higher dispersion. As the density of this system increases, the average intramolecular OH distance increases and the HOH angle decreases. The average permanent dipole moment $\bar{d}$ of water molecule in the BJH model increased from $\bar{d}^f$ = 1.86 D to 1.97 D. In our model of flexible molecules for $(O)_4(H_2O)_{50}$ aggregate, the value of $\bar{d}$ likewise increased from $\bar{d}^f$ = 1.85 D to 1.97 D.

Molecular-dynamic calculations were performed [22], and ab initio computations [23] were made for determining the structure of water clusters characterized by minimal energy. It was demonstrated that, as the cluster size increases, significant discrepancies are observed between the results obtained using different models. For example, for $(H_2O)_{20}$ cluster, the difference in energy between the most advantageous structures of POL1 [24] and SPC/E [6] models is 13.4%. The energy of $(H_2O)_{20}$ cluster in the model employed by us at T = 233 K takes an intermediate position between the respective energies for the POL1 and SPC/E models and is determined as –8.66 eV. The structures of clusters likewise differ significantly from one another. While a cluster in the form of a cell consisting of four-, five-, and six-link rings was obtained for the POL1 model, the structure with minimal energy for the SPC/E model is provided by a core formed by two molten pentagonal prisms. The minimal energy structure of $(H_2O)_{20}$ cluster for the model employed by us may be characterized as a highly distorted pentagonal dodecahedron. The introduction of polarizability and flexible bonds causes a decrease in energy of the system of stressed hydrogen bonds.

DIELECTRIC PROPERTIES

We will consider the case of scattering of nonpolarized light, where the molecular free path l is much less than the wavelength of light λ. The attenuation (extinction) coefficient h of incident beam may be determined both by the Rayleigh formula [25],

$$h = \frac{2\omega^4}{3\pi c^4}\frac{(\sqrt{\varepsilon}-1)^2}{N},$$

and in terms of the scattering coefficient ρ $\left(h = \frac{16\pi}{3}\rho\right)$ [26] in the approximation of scattering at an angle of 90°. Here, N is the number of scattering centers per cubic centimeter, c is the velocity of light, ε is the permittivity of the medium, and ω is the incident wave frequency.

In view of the fact that $h = \alpha + \rho$, where α is the absorption coefficient, we have

$$N = \frac{2\omega^4}{3\pi c^4}\frac{(\sqrt{\varepsilon}-1)^2}{\alpha}\left(1-\frac{3}{16\pi}\right).$$

We determine ultradisperse systems of the following types:

(1) a region filled with water clusters 10 to 50 molecules in size;

(2) a medium consisting of $(H_2O)_n$ clusters which absorbed a single O_2 molecule;

(3) a system consisting of $(O_2)_2(H_2O)_n$ aggregates;

(4) a set of $(H_2O)_n$ clusters which adsorbed two O atoms each; and

(5) a combination of $(O)_4(H_2O)_n$ formations.

In all instances, the step of variation of cluster size is $\Delta n = 5$. In order of sequence, we designate these systems by numbers I, II, III, IV, and V.

We form systems II–V so that the cluster containing i impurity molecules (atoms) and n water molecules would have the statistical weight

$$W_{in} = \frac{N_{in}}{N_\Sigma}, \quad i = 1(2)\ldots 2(4), \quad n = 10, 15, \ldots, 50,$$

where N_{in} is the number of clusters with i impurity molecules (atoms) and n water molecules per cubic centimeter, $N_\Sigma = \sum_{k=1}^{9} N_k$; and k characterizes the set of subscripts i, n. For example, at k = 1, the value of n is always 10, and i may have values of one, two, or four. Similar weights were used for $(H_2O)_n$ clusters which form system I. Thereafter, all of the spectral characteristics were calculated in view of the adopted statistical weights W_{in}.

The static dielectric constant ε_0 was calculated in terms of fluctuations of the total dipole moment [27], and the complex quantity $\varepsilon(\omega) = \varepsilon'(\omega) - i\varepsilon''(\omega)$ was determined in terms of the autocorrelation function of the total dipole moment of cluster [28, 29]. The absorption coefficient α of external IR radiation may be represented in terms of the imaginary part of frequency-dependent permittivity ε(ω) in the form [30]

$$\alpha(\omega) = 2\frac{\omega}{c}\mathrm{Im}[\varepsilon(\omega)^{1/2}].$$

The reflection coefficient R is defined as the ratio of average energy flux reflected from the surface to incident flow. In the case of normal incidence of plane

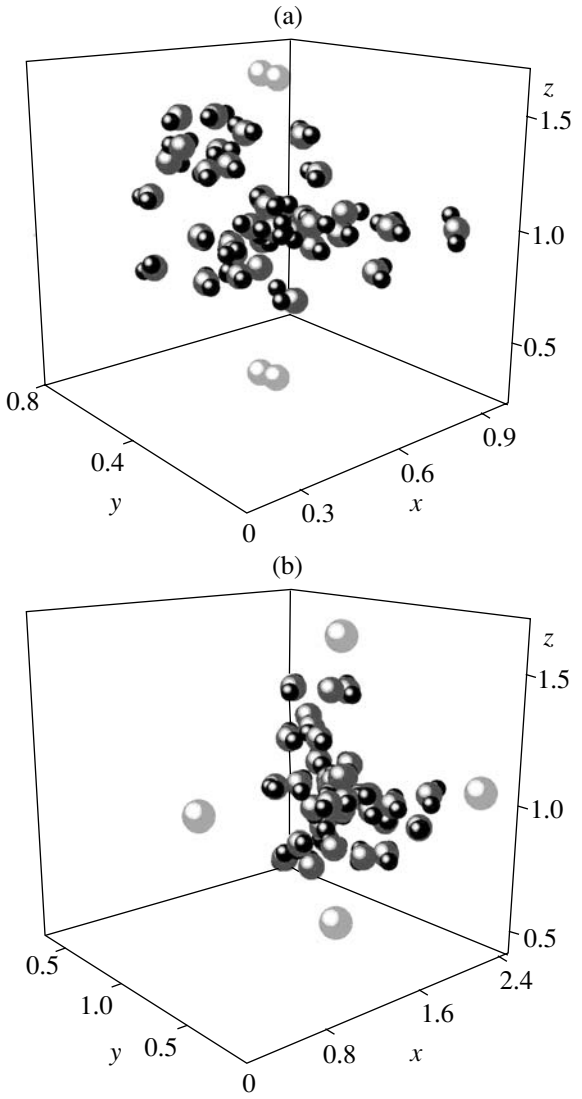

Fig. 3. Configurations of clusters: (a) $(O)_2(H_2O)_{40}$, (b) $(O)_4(H_2O)_{40}$, corresponding to the instant of time of 20 ps. The coordinates of molecules (atoms) are in nanometers.

monochromatic wave, the reflection coefficient is given by the formula [25]

$$R = \left| \frac{\sqrt{|\varepsilon_1|} - \sqrt{|\varepsilon_2|}}{\sqrt{|\varepsilon_1|} + \sqrt{|\varepsilon_2|}} \right|^2. \quad (1)$$

Here it is assumed that the wave incidence occurs from a transparent medium (medium 1) to a medium which may be both transparent and nontransparent, i.e., absorbing and scattering (medium 2). The subscripts used with permittivity in expression (1) indicate the medium.

The frequency dispersion of permittivity defines the frequency dependence of dielectric loss $P(\omega)$ in accordance with the expression [26]

$$P = \frac{\varepsilon'' \langle E^2 \rangle \omega}{4\pi},$$

where $\langle E^2 \rangle$ is the average value of square of electric field intensity, and ω is the frequency of emitted electromagnetic wave.

CALCULATION RESULTS

The molecules or atoms of oxygen were initially located at such a distance from $(H_2O)_n$ clusters that the interatomic spacings r_{OO} and r_{OH} between molecules of different sorts were at least 0.6 nm. Therefore, an O_2 molecule or an O atom, which experienced attraction, moved away from their initial position toward a water cluster and either stopped, and were then held at some distance from the cluster, or deposited directly on the cluster surface. The configuration of a water cluster, which consisted of 40 molecules and adsorbed two O_2 molecules, is given in Fig. 3a; the configuration of a similar cluster with four attached oxygen atoms is given in Fig. 3b. One can see that the orientation of O_2 molecules varied with time (the configuration relates to the instant of time of 20 ps), and the axes of O_2 molecules are directed along tangents to the cluster surface. This is associated with the attraction of each atom of O_2 molecule to the hydrogen atoms of neighboring water molecules, which are directed towards these atoms of O_2 molecule. Adsorbed O atoms partly attract some water molecules from the cluster; in so doing, the cluster retains its integrity. However, O_2 molecules and O atoms are encountered, which behave rather passively and neither are attracted to the surface nor move far away from the cluster. This is the manifestation of limited solubility of molecular and atomic oxygen in dispersed water medium.

The absorption coefficient α of IR radiation for disperse systems increases with frequency (Fig. 4). The $\alpha(\omega)$ spectra of disperse systems I–V have several maxima and minima. The strongest increase in the coefficient α of pure disperse water occurs in the frequency range from zero to 1000 cm^{-1}. Small weakly pronounced peaks are observed in this range at $\omega_1 = 215$ and $\omega_2 = 847$. For system II, the first two peaks at $\omega < 1000$ cm^{-1} turn out to be weakly separated; however, for systems III–V, they are already quite well resolved. In the absence of dissociation of oxygen captured by disperse systems, the values of the functions $\alpha(\omega)$ ascribed to these systems in the range $0 \le \omega \le 3500$ cm^{-1} periodically become higher or lower than the respective values for pure disperse water. The integral intensities of absorption of IR radiation by systems I–V correlate as 1 : 0.56 : 0.68 : 0.50 : 0.54. In the entire frequency range under consideration, the coefficient α decreases after adsorption of atomic oxygen by disperse water systems. It is only at the lowest frequencies $\omega < 350$ cm^{-1} that the presence of oxygen atoms in

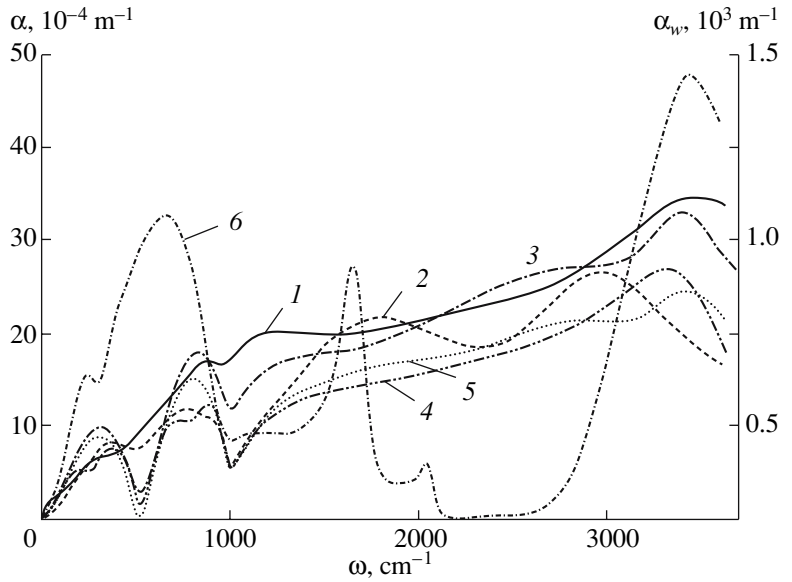

Fig. 4. The coefficient of absorption of IR radiation by systems of clusters: (*1*) system I, (*2*) II, (*3*) III, (*4*) IV, (*5*) V, (*6*) liquid water, experiment [31].

water clusters contributes to some increase in the absorption coefficient. A twofold increase in the concentration of atomic oxygen in water clusters gives an 8% increase in integral IR absorption for the respective disperse system III relative to system II. The principal maximum of the function $\alpha(\omega)$ for systems I–V is in the frequency range $3200 \le \omega \le 3410$ cm^{-1}. Curve *6* in Fig. 4 indicates the experimentally obtained IR radiation absorption spectrum $\alpha_w(\omega)$ of liquid water [31]. The spectrum is characterized by five maxima at frequencies of 200, 700, 1643, 2127, and 3407 cm^{-1}. The origin of the first maximum is explained by translational vibrations including the contributions by stretching (compression) and buckling of hydrogen bonds O–H…O [32]. The second peak is most likely associated with librations of molecules existing because of limitations due to neighboring hydrogen bonds. The third peak is largely due to deformation vibrations of molecules, and the fourth peak—to the interaction of deformation vibrations and librations.

The reflection coefficient R of plane monochromatic wave experiences significant variations after oxygen is trapped by water clusters (Fig. 5). The average value of reflection coefficient $\bar{R}$ decreases by 29% when a single O_2 molecule is attached to each water cluster, and by 53% when two O atoms are added to each water cluster. A twofold increase in the concentration of molecules and atoms in disperse systems causes a further decrease in the value of $\bar{R}$ by 52% and 27%, respectively. The $R(\omega)$ spectrum of pure disperse water has a large number of bursts with the principal maximum at $\omega = 1170$ cm^{-1}. The addition of molecular or atomic oxygen to clusters causes in the end the splitting of the $R(\omega)$ spectrum into bands. Even with a low concentration of impurity, the division of the $R(\omega)$ spectrum into seven peaks is observed (Fig. 5b), with some of these peaks splitting into two subpeaks (in the case of adsorption of atomic oxygen, all peaks are split). A twofold increase in the concentration of oxygen contained in the clusters leads to the smoothing of peaks, splitting disappears, and the locations of peaks are retained.

The $P(\omega)$ power spectra, which represent the rate of scattering of energy by disperse systems, are given in Fig. 6a. One or two characteristic peaks corresponding to the increase in dissipation of energy for both system I and systems II–V are observed in the initial part of the $P(\omega)$ spectrum, i.e., at $\omega < 1000$ cm^{-1}. In so doing, the maximal intensity of IR radiation for system I is higher than that for systems II and III but lower than that for systems IV and V. A significant increase in radiation power for systems binding atomic oxygen (IV and V) is observed in the frequency range $\omega > 1000$ cm^{-1}. By and large, the increase in power P with frequency for pure disperse water occurs much faster than for disperse water systems holding molecular oxygen but much slower than for systems enriched with atomic oxygen. The highest rate of dissipation of energy stored by systems I–V is realized at frequencies of 3470, 2720, 3180, 3130, and 3350 cm^{-1}, respectively. The maximal values of power of radiation of systems I–V correlate as 1 : 0.29 : 0.13 : 2.55 : 1.79. Therefore, the dissociation of oxygen adsorbed by water clusters leads to a significant acceleration of dissipation of thermal energy, especially, in the frequency range $1000 \le \omega \le 3500$ cm^{-1}. Figure 6b shows the maximal power of IR radiation as a function of the number of water molecules in a cluster. One can see that the fastest dissipation of energy is

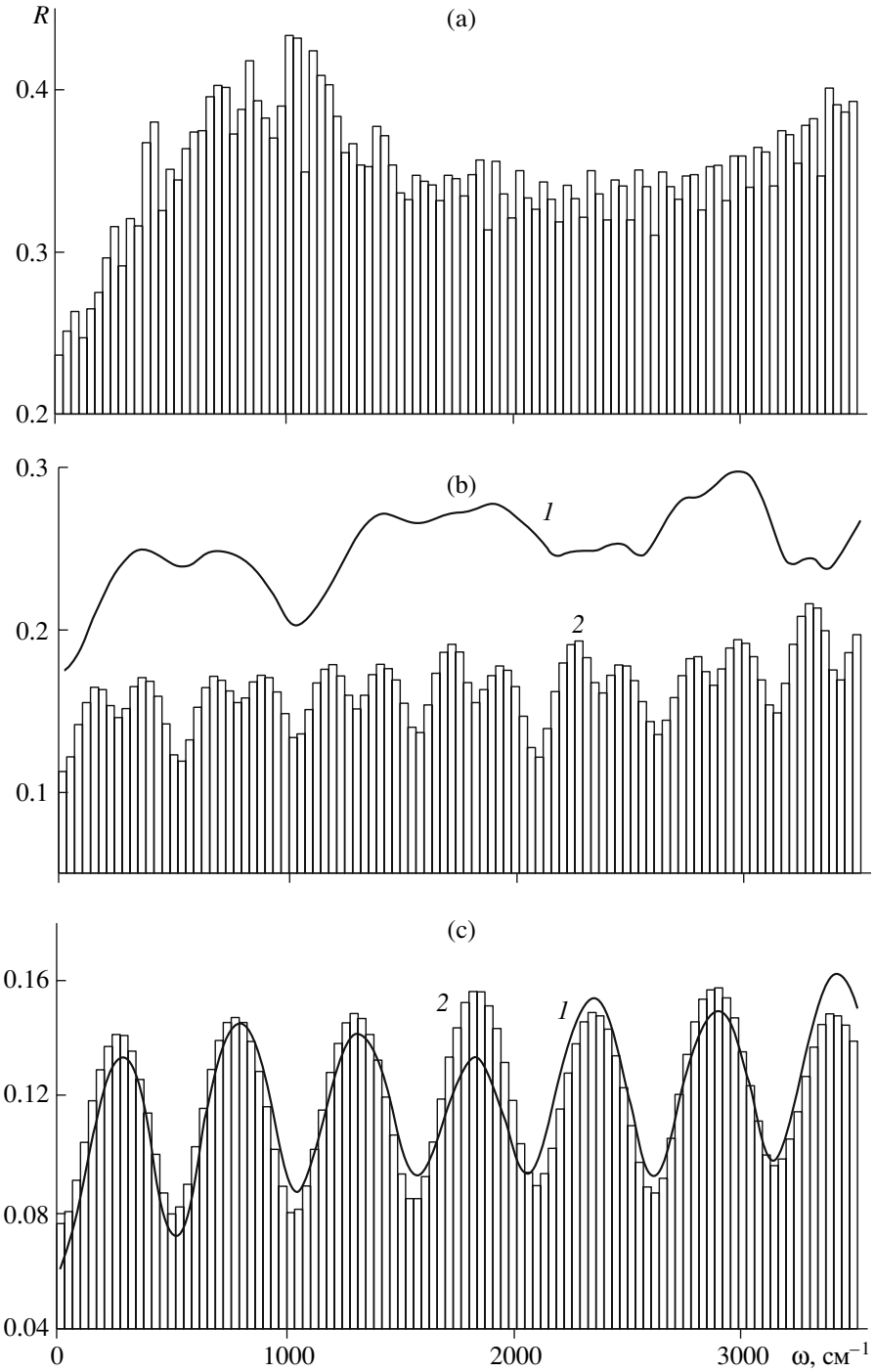

Fig. 5. The coefficient of reflection of plane monochromatic electromagnetic wave by systems of clusters: (a) system I; (b) systems (*1*) II, (*2*) IV; (c) systems (*1*) III, (*2*) V.

characteristic of $(O)_2(H_2O)_{40}$ and $(O)_4(H_2O)_{35}$ clusters which hold atomic oxygen; in so doing, the power P for $(O)_2(H_2O)_{40}$ cluster is higher than that for $(O)_4(H_2O)_{35}$ aggregate. Of pure water clusters, the highest power of thermal radiation is exhibited by $(H_2O)_{20}$ cluster, and of clusters which adsorbed molecular oxygen—by $(O_2)_2(H_2O)_{50}$ cluster.

CONCLUSIONS

The oxygen fraction in atmospheric air is 20.96%. The dissolution of natural mixture of air-forming gases in water results in a 34.4% concentration of O_2. Oxygen is soluble in water to a greater extent than nitrogen but to a smaller extent than carbon dioxide or argon. When

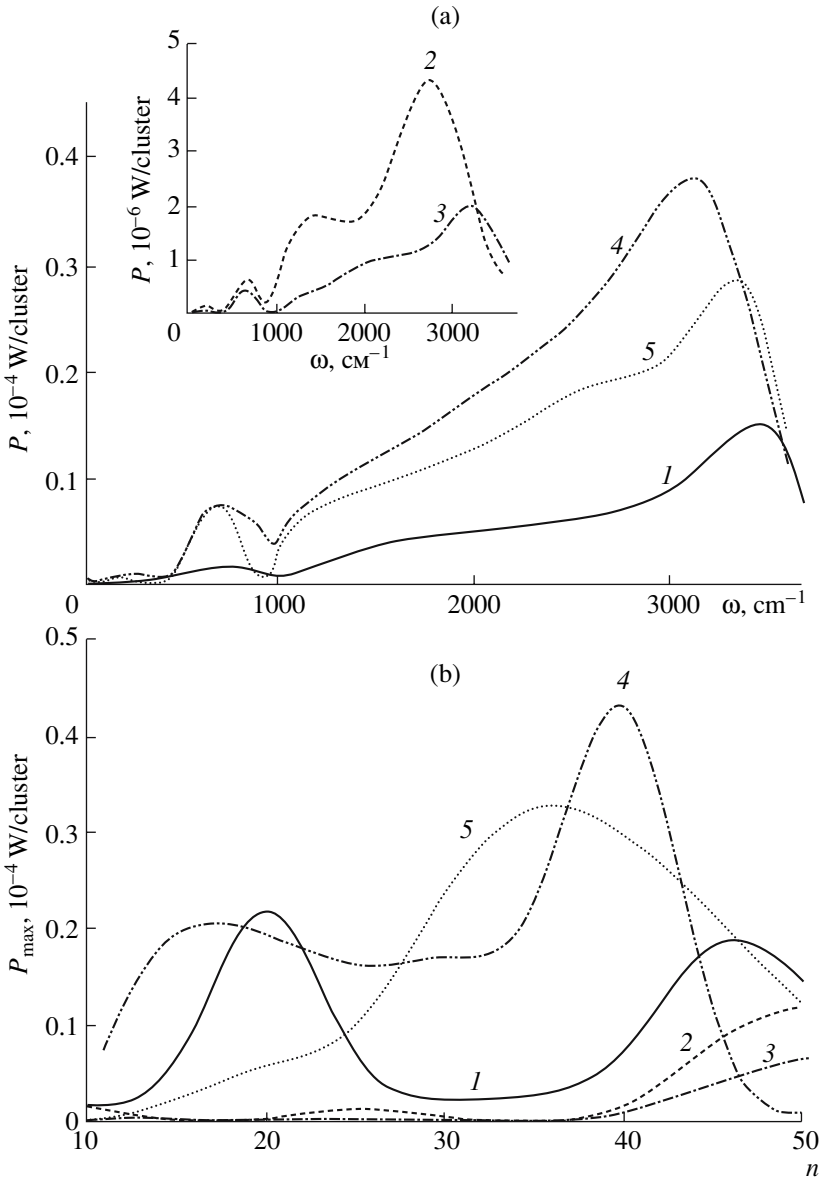

Fig. 6. (a) The power of scattering of IR radiation by systems of clusters: (*1*) system I, (*2*) II, (*3*) III, (*4*) IV, (*5*) V; and (b) the maximal rate of scattering of energy as a function of the number of water molecules n in clusters: (*1*) $(H_2O)_n$, (*2*) $O_2(H_2O)_n$, (*3*) $(O_2)_2(H_2O)_n$, (*4*) $(O)_2(H_2O)_n$, (*5*) $(O)_4(H_2O)_n$.

dissolved in water, oxygen may change from the molecular to atomic state.

The flexible model of water molecules employed by us turned out to be largely suitable for the description of adsorption of oxygen by water clusters. The presence of adsorbed molecules and atoms of oxygen in the sphere of effect of the forces of intermolecular interaction causes a reduction (up to 5%) of the most probable magnitude of OH bond in the molecule. In so doing, the intramolecular deformation vibrations produce a variation of the HOH angle within 10°. The MCDHO and BJH models for pure water are characterized by a much wider range of variation of the HOH angle (up to 20°). When the valence angle decreases by 20°, the intramolecular energy of Coulomb interaction increases by 18.1%; when the HOH angle decreases by 10°, this energy increases by only 8.1%. As a result, the coefficient of absorption of IR radiation α in the vibration frequency range of zero to 3500 cm^{-1} as a rule increases with frequency and reaches its principal maximum in the frequency range $3200 \le \omega \le 3410$ cm^{-1}. As the molecular oxygen concentration increases, the coefficient α of disperse water system decreases; when the atomic oxygen concentration increases at certain frequencies (for example, in the frequency range $1140 \le \omega \le 2880$ cm^{-1}), the value of α_V exceeds the values of α_{IV}.

The reflection of plane monochromatic electromagnetic wave by disperse systems decays with increasing fraction of adsorbed oxygen and is accompanied by variation of the wave phase by π, because the correlation $|\varepsilon_2| > |\varepsilon_1|$ remains valid throughout the interval $0 \le \omega \le 3500$ cm^{-1}. The emergence of additional O_2 molecules or O atoms in disperse systems results in the splitting of the $R(\omega)$ spectrum into bands. The capture of molecular oxygen by a disperse water system resulted in a significant decrease in the rate of dissipation P of the energy accumulated by clusters; the absorption of atomic oxygen, on the contrary, was accompanied by a significant increase in P.

Therefore, the adsorption of oxygen by disperse water systems leads to a decay of the absorption and reflection of IR radiation by these systems. The rate of dissipation of the energy received by clusters decreases when the clusters capture molecular oxygen and increases when the oxygen in the clusters is in the atomic state. By and large, oxygen dissolved in atmospheric moisture causes a decrease in the greenhouse effect due to disperse medium, i.e., produces antigreenhouse effect.

ACKNOWLEDGMENTS

This study was supported by the Russian Foundation for Basic Research (grant no. 04-02-17322).

REFERENCES

1. Snow, G.E. and Javor, G.T., *Origins*, 1975, vol. 2, p. 59.
2. Chibowski, E., Holysz, L., Szczes, A., and Chibowski, M., *Water Sci. Technol.*, 2004, vol. 49, p. 169.
3. Gruenlon, C.J., Carney, J.R., Hagemeister, F.C. et al., *J. Chem. Phys.*, 2000, vol. 113, p. 2290.
4. Galashev, A.E., Chukanov, V.N., and Galasheva, O.A., *Kolloidn. Zh.*, 2006, vol. 68, no. 2, p. 155.
5. Berendsen, H.J.C., Postma, J.P.M., Gunsteren, W.F., and Hermans, J., in *Intermolecular Forces*, Pullman, B., Ed., Dordrecht: Reidel, 1981, p. 331.
6. Berendsen, H.J.C., Grigera, J.R., and Straatsma, T.P., *J. Phys. Chem.*, 1987, vol. 91, p. 6269.
7. Jorgensen, W.L., Chandrasekhar, J., Madura, J.D. et al., *J. Chem. Phys.*, 1983, vol. 79, p. 926.
8. Dang, L.X. and Chang, T.-M., *J. Chem. Phys.*, 1997, vol. 106, p. 8149.
9. Galashev, A.E., Rakhmanova, O.R., and Chukanov, V.N., *Khim. Fiz.*, 2005, vol. 24, no. 3, p. 90.
10. Spackman, M.A., *J. Chem. Phys.*, 1986, vol. 85, p. 6579.
11. Spackman, M.A., *J. Chem. Phys.*, 1986, vol. 85, p. 6587.
12. Saint-Martin, H., Hess, B., and Berendsen, H.J.C., *J. Chem. Phys.*, 2004, vol. 120, p. 11 133.
13. Lemberg, H.L. and Stillinger, F.H., *J. Chem. Phys.*, 1975, vol. 62, p. 1677.
14. Rahman, A., Stillinger, F.H., and Lemberg, H.L., *J. Chem. Phys.*, 1975, vol. 63, p. 5223.
15. Haile, J.M., *Molecular Dynamics Simulation. Elementary Methods*, New York: Wiley, 1992.
16. Koshlyakov, V.N., *Zadachi dinamiki tverdogo tela i prikladnoi teorii giroskopov* (Problems in Dynamics of Solids and Applied Theory of Gyroscopes), Moscow: Nauka, 1985.
17. Sonnenschein, R., *J. Comput. Phys.*, 1985, vol. 59, p. 347.
18. Kalinichev, A.G. and Heinzinger, K., *Geochim. Cosmochim. Acta*, 1995, vol. 59, p. 641.
19. Farber, D.L., Williams, Q., and Knittle, E., *EOS Trans. Am. Geophys. Union, 1990, vol. 71, p. 1600.*
20. Kohl, W., Lindner, H.A., and Franck, E.U., *Ber. Bunsenges. Phys. Chem.*, 1991, vol. 95, p. 1586.
21. Stem, H.A. and Berne, B.J., *J. Chem. Phys.*, 2001, vol. 115, p. 7622.
22. Sremaniak, L.S., Perera, L., and Berkowitz, M.L., *J. Chem. Phys.*, 1996, vol. 105, no. 9, p. 3715.
23. Tsai, C.J. and Jordan, K.D., *J. Phys. Chem.*, 1993, vol. 97, p. 5207.
24. Dang, L.X. and Garrett, B.C., *J. Chem. Phys.*, 1993, vol. 99, p. 2972.
25. Landau, L.D. and Lifshitz, E.M., *Elektrodinamika sploshnykh sred* (Electrodynamics of Continuous Media), Moscow: Nauka, 1982, vol. 8.
26. *Fizicheskaya entsiklopediya. T. 1* (Physical Encyclopedia), Prokhorov, A.M., Ed., Moscow: Sovetskaya Entsiklopediya, 1988, p. 702.
27. Bresme, F., *J. Chem. Phys.*, 2001, vol. 115, p. 7564.
28. Neumann, M., *J. Chem. Phys.*, 1985, vol. 82, p. 5663.
29. Bosma, W.B., Fried, L.E., and Mukamel, S., *J. Chem. Phys.*, 1993, vol. 98, p. 4413.
30. Neumann, M., *J. Chem. Phys.*, 1986, vol. 85, p. 1567.
31. Goggin, P.L. and Carr, C., Far Infrared Spectroscopy and Aqueous Solutions, in *Water and Aqueous Solutions*, Bristol-Boston: Adam Hilger, 1986, vol. 37, p. 149.
32. van der Maas, J.H., *Basic Infrared Spectroscopy*, London: Pitman Press, 1969.